

## Synthesis and Structural Characterisation of a Novel High-nuclearity Gold–Tin Cluster Compound, $[\text{Au}_8(\text{PPh}_3)_7(\text{SnCl}_3)]_2[\text{SnCl}_6]^+$

Zenon Demidowicz, Roy L. Johnston, Jonathan C. Machell, D. Michael P. Mingos,\* and Ian D. Williams

*Inorganic Chemistry Laboratory, University of Oxford, South Parks Road, Oxford OX1 3QR*

The compound  $[\text{Au}_8(\text{PPh}_3)_7(\text{SnCl}_3)]_2[\text{SnCl}_6]$  has been synthesised from either  $[\text{Au}_8(\text{PPh}_3)_7][\text{NO}_3]_2$  or  $[\text{Au}_9(\text{PPh}_3)_8][\text{NO}_3]_3$  and excess of  $\text{SnCl}_2 \cdot 2\text{H}_2\text{O}$  in acetone solution. Alternatively it can be synthesised in high yield from  $[\text{Au}_8(\text{PPh}_3)_8][\text{NO}_3]_2$  and  $\text{NEt}_4\text{SnCl}_3$  in acetone. The compound has been characterised by  $^{31}\text{P}\{-^1\text{H}\}$  n.m.r. and  $^{119}\text{Sn}$  Mössbauer spectroscopy and a single-crystal X-ray crystallographic determination. It crystallises in the monoclinic space group  $C2/c$  with  $a = 48.230(14)$ ,  $b = 16.831(7)$ ,  $c = 32.240(10)$  Å, and  $\beta = 96.50(3)^\circ$ . The geometry of the gold atoms in the cluster closely resembles that observed previously in  $[\text{Au}_8(\text{PPh}_3)_7]^{2+}$  and corresponds to a fragment of a centred icosahedron. The  $\text{SnCl}_3$  ligand is co-ordinated only to the central gold atom, with  $\text{Au}\text{--}\text{Sn}$  2.625(3) Å, and does not interact significantly with the surface gold atoms to complete a hemispherical polyhedron. The distances from the central gold atom to those gold atoms on the surface lie in the range 2.633(2)—2.679(2) Å and are shorter than the distances between the surface gold atoms [2.847(2)—2.965(3) Å]. The relationship between the structure of  $[\text{Au}_8(\text{PPh}_3)_7(\text{SnCl}_3)]^+$  and those of related high-nuclearity gold cluster compounds with toroidal and spherical topologies has been explored using molecular-orbital calculations.

Although a rich structural chemistry has developed as a result of the study of high-nuclearity gold cluster compounds<sup>1–3</sup> the reactions of these compounds have not been extensively studied. Some substitution reactions with isocyanides and chelating phosphine ligands have been investigated,<sup>4,5</sup> and cluster degradation and aggregation reactions promoted by either phosphine or halide ligands have been identified.<sup>6,7</sup> The synthesis of mixed-metal cluster compounds based on these high-nuclearity precursors has received little attention. The reported synthesis of  $[\text{Au}_6(\text{PPh}_3)_4\{\text{Co}(\text{CO})_4\}_2]$  from  $[\text{Au}_8(\text{PPh}_3)_7]^{2+}$  and  $[\text{Co}(\text{CO})_4]^-$ <sup>8</sup> has not been extended to other redox condensation processes based on alternative metal carbonyl anions. In addition although there were some early reports of gold–tin cluster compounds, e.g.  $[\text{Au}_5(\text{PPh}_3)_4(\text{SnCl}_3)]$  and  $[\text{Au}_3(\text{PPh}_3)_2(\text{SnI}_3)]$ , their formulations depended primarily on analytical data and there has been no systematic effort to characterise such compounds by modern spectroscopic and structural techniques.<sup>9</sup> In this paper we describe the synthesis and structural characterisation of the first example of a high-nuclearity gold–tin cluster compound.

### Results and Discussion

The compound  $[\text{Au}_8(\text{PPh}_3)_7(\text{SnCl}_3)]_2[\text{SnCl}_6]$  (**1**) was obtained in high yield either from  $[\text{Au}_9(\text{PPh}_3)_8][\text{NO}_3]_3$  or  $[\text{Au}_8(\text{PPh}_3)_7][\text{NO}_3]_2$ <sup>10,11</sup> and an excess of  $\text{SnCl}_2 \cdot 2\text{H}_2\text{O}$  in acetone. It has also been synthesised directly from  $\text{NEt}_4^+\text{SnCl}_3^-$  and  $[\text{Au}_8(\text{PPh}_3)_8][\text{NO}_3]_2$  in acetone. The  $^{31}\text{P}\{-^1\text{H}\}$  n.m.r. spectrum of (**1**) in  $\text{CHCl}_2\text{CHCl}_2$  showed the presence of a singlet at 51.02 p.p.m. relative to trimethyl phosphate flanked symmetrically by two pairs of low-intensity satellites with the relative intensities 17:178:17, which is consistent with the presence of a single tin atom ( $^{119}\text{Sn}$ ,  $I = \frac{1}{2}$ , 8.58% abundance;  $^{117}\text{Sn}$ ,  $I = \frac{1}{2}$ , 7.61% abundance) coupling equally to all the phosphorus atoms [ $^3J(^{31}\text{P}\text{--}^{119}\text{Sn}) = 371$ ,  $^3J(^{31}\text{P}\text{--}^{117}\text{Sn}) =$

**Table 1.** Experimental details for the crystal structure determination of  $[\text{Au}_8(\text{PPh}_3)_7(\text{SnCl}_3)]_2[\text{SnCl}_6]$

|  |  |
|--|--|
| Formula  | $\text{C}_{252}\text{H}_{210}\text{Au}_{16}\text{Cl}_{12}\text{P}_{14}\text{Sn}_3$ |
| Space group                                      | $C2/c$ (no. 15)  |
| $a/\text{Å}$                                     | 48.230(14)   |
| $b/\text{Å}$                                     | 16.831(7)  |
| $c/\text{Å}$                                     | 32.240(10)   |
| $\beta/^\circ$                                   | 96.50(3)   |
| $U/\text{Å}^3$                                   | 25 999   |
| $Z$  | 4  |
| $D_c/\text{g cm}^{-3}$                           | 1.94   |
| Dimensions (mm)                                  | $0.40 \times 0.35 \times 0.10$   |
| $\mu(\text{Mo}\text{--}K_\alpha)/\text{cm}^{-1}$ | 95.1   |
| Scan technique                                   | $\omega\text{--}2\theta$   |
| Scan width ( $^\circ$ )                          | $0.9 + 0.35 \tan \theta$   |
| Max. scan time (s)                               | 60   |
| Crystal decay (%)                                | 33   |
| Total reflections                                | 11 747   |
| $2\theta$ range ( $^\circ$ )                     | 3–45   |
| Observed reflections: [ $I > 3\sigma(I)$ ]       | 4 492  |
| $R$ -merge                                       | 0.0376   |
| Max. and min. absorption correction              | 1.8, 1.0   |
| No. least-squares parameters                     | 405  |
| Weighting scheme coefficients                    | 6.479, $-2.152$ , 4.288  |
| $R$  | 0.0547   |
| $R'$   | 0.0633   |

354 Hz]. The spectrum retained the same characteristics even down to 180 K, but in view of the well documented stereochemical non-rigidity of gold cluster compounds this result could not be interpreted unambiguously in terms of a structure with all the phosphorus atoms in chemically equivalent environments.<sup>12</sup> The  $^{119}\text{Sn}$  Mössbauer spectrum was interpreted in terms of two overlapping resonances:  $\delta$  0.32,  $\Delta\epsilon_Q = 0$ ,  $\Gamma$  1.61  $\text{mm s}^{-1}$ ;  $\delta$  2.18,  $\Delta\epsilon_Q$  1.39,  $\Gamma_1 = 0.86$ , and  $\Gamma_2 = 0.85$   $\text{mm s}^{-1}$ . The former is assigned to the  $[\text{SnCl}_6]^{2-}$  anion and the latter to the  $\text{SnCl}_3$  ligand. The  $[\text{SnCl}_6]^{2-}$  anion is generally observed at approximately 0.49  $\text{mm s}^{-1}$  (relative to  $\text{SnO}_2$ )<sup>13</sup> but the isomer shift difference can be attributed either to lack of resolution associated with the overlapping peaks or differences resulting from the unusually large nature of the

† Supplementary data available: see Instructions for Authors, *J. Chem. Soc., Dalton Trans.*, 1988, Issue 1, pp. xvii–xx.

Non-S.I. unit employed: eV  $\approx 1.60 \times 10^{-19}$  J.

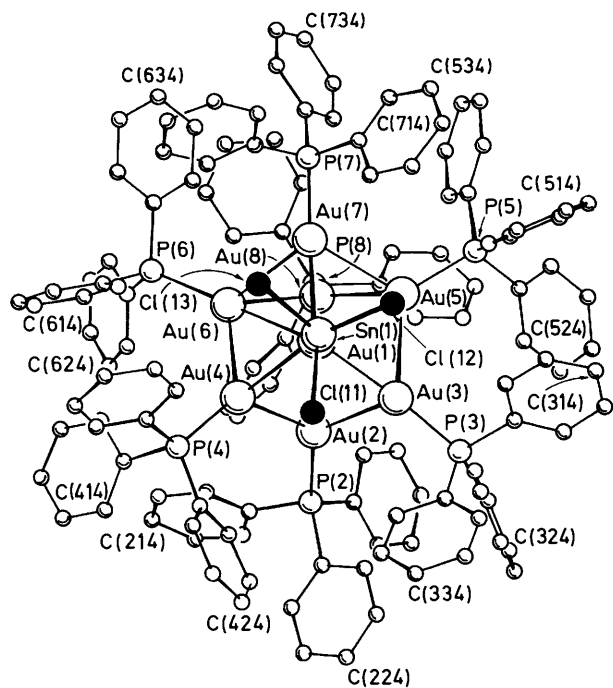
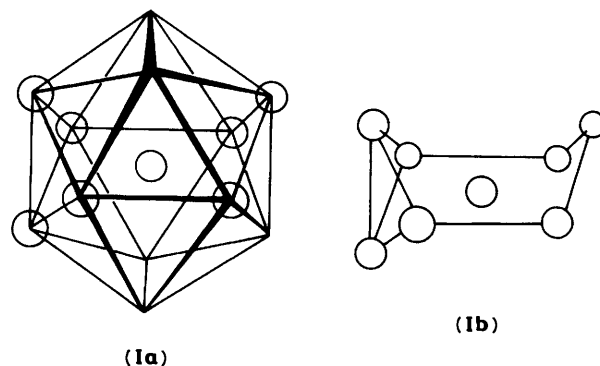


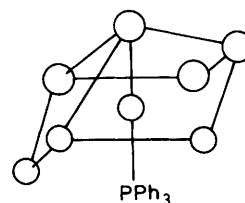
Figure 1. Illustration of the molecular structure of the cation in  $[\text{Au}_8(\text{PPh}_3)_7(\text{SnCl}_3)]_2[\text{SnCl}_6]$  viewed in the direction of the Sn-Au(1) (interstitial) bond



(Ia)

(Ib)

$[\text{Au}_8(\text{PPh}_3)_7]^{2+}$  skeleton



$[\text{Au}_8(\text{PPh}_3)_8]^{2+}$  (II)

Scheme 1.

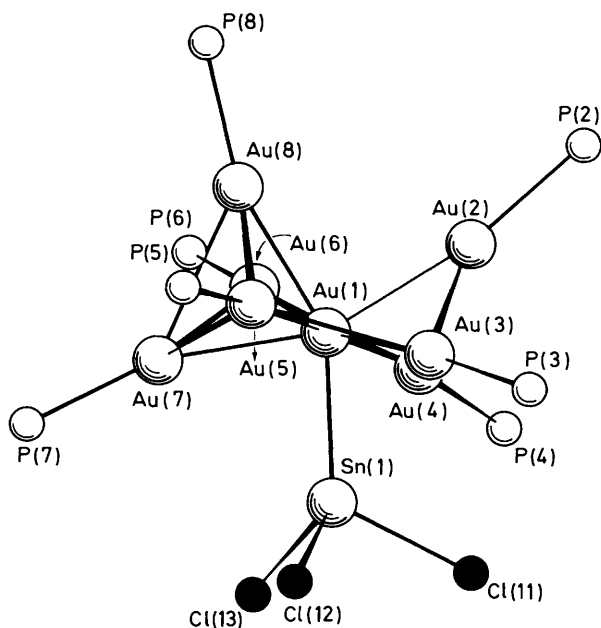


Figure 2. Illustration of the molecular structure of the  $[\text{Au}_8(\text{PPh}_3)_7(\text{SnCl}_3)]^+$  cation with the phenyl rings omitted. The view is perpendicular to that shown in Figure 1

accompanying cation. The quadrupole-split doublet has an isomer shift and quadrupole splitting similar to that reported previously for  $[\text{Au}(\text{PPh}_3)_3(\text{SnCl}_3)]^+$ .<sup>14</sup> In order to confirm the molecular structure of (1) a single-crystal X-ray crystallographic determination was undertaken.

The details of the X-ray crystallographic determination are summarised in Table 1 and the Experimental section. The positional parameters are summarised in Table 2 and the important bond lengths and angles in Table 3. Alternative views

of the structure with and without the phenyl rings are illustrated in Figures 1 and 2.

The gold atoms in the structure define a geometry which can be described either in terms of a fragment of an icosahedron or in terms of a centred hexagonal chair (see Scheme 1). The latter is defined by the atoms Au(2) to Au(7) in Figure 2, which are all bonded to the central gold atom Au(1). In addition Au(8) is bonded to Au(1), Au(5), Au(6), and Au(7). A similar metal-cage geometry has been observed previously for  $[\text{Au}_8(\text{PPh}_3)_7]^{2+}$ .<sup>15</sup> The distances from the central gold atom to the peripheral gold atoms lie in the range 2.633(2)–2.679(2) Å. In contrast the gold-gold bond lengths for the peripheral gold atoms lie in the range 2.847(2)–2.965(3) Å. The relative shortening of the radial gold-gold bond lengths is a common feature of high-nuclearity gold cluster compounds.<sup>1</sup> In  $[\text{Au}_8(\text{PPh}_3)_7][\text{NO}_3]_2$  the radial metal-metal bond lengths lie between 2.63(1) and 2.72(1) Å and the peripheral ones between 2.80(1) and 2.94(1) Å, except for Au(7)–Au(8) 2.71(1) Å.<sup>15</sup>

In  $[\text{Au}_8(\text{PPh}_3)_7(\text{SnCl}_3)]^+$  (1) the  $\text{SnCl}_3$  group is coordinated exclusively to the central gold atom, Au(1), with Au–Sn 2.625(3) Å. This distance is significantly shorter than the Au–Sn bond length of 2.881(1) Å reported for  $[\text{Au}(\text{PMe}_2\text{Ph})_2(\text{SnCl}_3)]^+$ <sup>16</sup> which has also been described as a strong ion pair,  $[\text{Au}(\text{PMe}_2\text{Ph})_2]^+\text{SnCl}_3^-$ . The contacts between Sn and the peripheral gold atoms which define the hexagonal chair are greater than 3.333(5) Å and therefore are classified as non-bonding. The compound  $[\text{Au}_8(\text{PPh}_3)_8]^{2+}$ <sup>17,18</sup> also has a geometry based on a centred hexagonal chair with the Au–PPh<sub>3</sub> moiety bonded axially to the central gold atom and Au–Au 2.635(5) Å. The contacts between this gold atom and the three nearest gold atoms of the hexagonal chair lie between 2.909(5) and 2.960(5) Å. The Sn–Cl bond lengths in the present compound lie between 2.40(1) and 2.46(1) Å and the Cl–Sn–Cl bond angles between 95.7 and 97.1°. These bond lengths and angles fall in the ranges generally associated with co-ordinated  $\text{SnCl}_3$ .<sup>19</sup>

**Table 2.** Positional parameters ( $\times 10^{-4}$ ) for  $[\text{Au}_8(\text{PPh}_3)_7(\text{SnCl}_3)_2][\text{SnCl}_6]$ 

| Atom   | X/a        | Y/b        | Z/c        | Atom   | X/a       | Y/b        | Z/c       |
|--------|------------|------------|------------|--------|-----------|------------|-----------|
| Au(1)  | 1 494.5(3) | 769.6(9)   | 4 081.6(5) | C(415) | 976(7)    | -3 766(14) | 4 541(11) |
| Au(2)  | 1 512.1(4) | -414(1)    | 3 544.6(6) | C(416) | 1 216(5)  | -3 300(19) | 4 590(10) |
| Au(3)  | 1 952.0(3) | 733(11)    | 3 703.4(5) | C(421) | 1 793(6)  | -2 420(19) | 4 661(13) |
| Au(4)  | 1 453.4(3) | -661(1)    | 4 422.0(5) | C(422) | 1 814(8)  | -2 527(25) | 4 237(11) |
| Au(5)  | 1 604.3(3) | 2 144(1)   | 3 719.0(5) | C(423) | 2 038(10) | -2 969(28) | 4 109(9)  |
| Au(6)  | 1 012.3(3) | 471(1)     | 4 363.9(6) | C(424) | 2 241(7)  | -3 304(21) | 4 404(14) |
| Au(7)  | 1 285.3(3) | 2 033(1)   | 4 443.4(6) | C(425) | 2 220(7)  | -3 198(19) | 4 828(12) |
| Au(8)  | 1 061.9(4) | 1 380(1)   | 3 618.7(6) | C(426) | 1 996(7)  | -2 756(20) | 4 956(9)  |
| Sn(1)  | 1 871.5(6) | 851(2)     | 4 735(1)   | C(431) | 1 558(7)  | -1 780(20) | 5 351(8)  |
| Cl(11) | 2 198(2)   | -240(7)    | 4 853(4)   | C(432) | 1 719(6)  | -1 149(17) | 5 523(10) |
| Cl(12) | 2 218(2)   | 1 881(7)   | 4 802(4)   | C(433) | 1 770(6)  | -1 067(17) | 5 955(11) |
| Cl(13) | 1 752(3)   | 954(8)     | 5 455(4)   | C(434) | 1 659(7)  | -1 615(21) | 6 215(8)  |
| Sn(2)  | 5 000      | 359(6)     | 2 500      | C(435) | 1 498(7)  | -2 246(18) | 6 043(10) |
| Sn(3)  | 4 827(3)   | 1 044(9)   | 3 308(5)   | C(436) | 1 448(6)  | -2 329(16) | 5 611(11) |
| Cl(21) | 5 000      | -1 046(19) | 2 500      | C(511) | 2 009(5)  | 3 833(16)  | 3 713(9)  |
| Cl(22) | 5 000      | 1 796(23)  | 2 500      | C(512) | 2 113(6)  | 4 517(17)  | 3 539(7)  |
| Cl(23) | 5 214(7)   | 305(17)    | 3 254(9)   | C(513) | 2 344(6)  | 4 911(14)  | 3 747(10) |
| Cl(24) | 4 537(7)   | 317(17)    | 2 790(11)  | C(514) | 2 471(5)  | 4 621(19)  | 4 129(10) |
| Cl(31) | 4 719(12)  | -187(27)   | 3 632(16)  | C(515) | 2 366(7)  | 3 937(21)  | 4 303(8)  |
| Cl(32) | 4 933(14)  | 2 269(31)  | 2 953(18)  | C(516) | 2 135(7)  | 3 543(15)  | 4 096(10) |
| Cl(33) | 5 240(12)  | 422(40)    | 3 082(20)  | C(521) | 1 775(6)  | 3 259(18)  | 2 899(7)  |
| Cl(34) | 4 568(15)  | 577(43)    | 2 653(19)  | C(522) | 1 693(6)  | 3 827(15)  | 2 592(10) |
| Cl(35) | 5 094(8)   | 1 482(24)  | 3 959(12)  | C(523) | 1 782(6)  | 3 757(17)  | 2 195(9)  |
| Cl(36) | 4 430(12)  | 1 654(40)  | 3 521(21)  | C(524) | 1 954(6)  | 3 120(19)  | 2 105(8)  |
| P(2)   | 1 454(2)   | -1 351(7)  | 3 027(4)   | C(535) | 2 036(6)  | 2 552(16)  | 2 411(10) |
| P(3)   | 2 374(2)   | 591(7)     | 3 447(4)   | C(526) | 1 947(6)  | 2 622(16)  | 2 808(9)  |
| P(4)   | 1 508(2)   | -1 842(7)  | 4 786(4)   | C(531) | 1 421(5)  | 4 044(17)  | 3 409(10) |
| P(5)   | 1 705(2)   | 3 347(7)   | 3 439(4)   | C(532) | 1 174(7)  | 3 859(15)  | 3 160(9)  |
| P(6)   | 596(2)     | 248(7)     | 4 614(4)   | C(533) | 955(5)    | 4 410(21)  | 3 111(9)  |
| P(7)   | 1 222(2)   | 3 063(7)   | 4 883(4)   | C(534) | 982(6)    | 5 147(18)  | 3 312(11) |
| P(8)   | 706(3)     | 1 533(8)   | 3 104(4)   | C(535) | 1 229(8)  | 5 333(15)  | 3 561(10) |
| C(211) | 1 153(5)   | -1 199(17) | 3 061(10)  | C(536) | 1 448(6)  | 4 781(20)  | 3 610(9)  |
| C(212) | 1 076(6)   | -2 130(17) | 3 460(8)   | C(611) | 635(6)    | -354(17)   | 5 082(8)  |
| C(213) | 846(6)     | -2 607(18) | 3 512(9)   | C(612) | 435(5)    | -896(18)   | 5 184(9)  |
| C(214) | 692(5)     | -2 953(18) | 3 165(12)  | C(613) | 486(7)    | -1 357(17) | 5 543(11) |
| C(215) | 769(7)     | -2 822(21) | 2 767(9)   | C(614) | 735(8)    | -1 275(20) | 5 800(9)  |
| C(216) | 999(7)     | -2 345(21) | 2 715(8)   | C(615) | 935(5)    | -733(21)   | 5 699(10) |
| C(221) | 1 743(5)   | -2 061(17) | 3 007(9)   | C(616) | 885(5)    | -272(17)   | 5 340(11) |
| C(222) | 1 703(5)   | -2 879(19) | 2 965(10)  | C(621) | 332(5)    | -240(17)   | 4 255(9)  |
| C(223) | 1 931(7)   | -3 380(13) | 2 942(11)  | C(622) | 59(6)     | 37(14)     | 4 178(9)  |
| C(224) | 2 119(6)   | -3 064(19) | 2 962(11)  | C(623) | -135(4)   | -374(19)   | 3 904(10) |
| C(225) | 2 240(5)   | -2 247(21) | 3 004(10)  | C(624) | -57(6)    | -1 062(19) | 3 706(9)  |
| C(226) | 2 011(6)   | -1 745(14) | 3 026(10)  | C(625) | 216(7)    | -1 339(15) | 3 782(10) |
| C(231) | 1 395(7)   | -946(20)   | 2 507(9)   | C(626) | 411(5)    | -928(18)   | 4 057(10) |
| C(232) | 1 497(6)   | -1 303(16) | 2 165(12)  | C(631) | 433(6)    | 1 158(14)  | 4 759(10) |
| C(233) | 1 448(8)   | -955(24)   | 1 769(10)  | C(632) | 411(6)    | 1 800(19)  | 4 485(7)  |
| C(234) | 1 297(8)   | -249(24)   | 1 716(9)   | C(633) | 287(6)    | 2 503(15)  | 4 597(9)  |
| C(235) | 1 196(7)   | 108(17)    | 2 057(13)  | C(634) | 186(6)    | 2 564(15)  | 4 983(11) |
| C(236) | 1 244(7)   | -240(20)   | 2 453(10)  | C(635) | 208(6)    | 1 922(20)  | 5 257(8)  |
| C(311) | 2 582(6)   | 1 466(17)  | 3 471(12)  | C(636) | 332(6)    | 1 219(16)  | 5 145(9)  |
| C(312) | 2 618(7)   | 1 851(23)  | 3 856(9)   | C(711) | 1 511(7)  | 3 720(26)  | 4 988(12) |
| C(313) | 2 786(8)   | 2 525(23)  | 3 907(11)  | C(712) | 1 490(7)  | 4 544(28)  | 4 929(14) |
| C(314) | 2 918(8)   | 2 814(20)  | 3 574(16)  | C(713) | 1 729(11) | 5 013(18)  | 4 979(14) |
| C(315) | 2 881(8)   | 2 428(27)  | 3 189(13)  | C(714) | 1 989(8)  | 4 659(27)  | 5 089(12) |
| C(316) | 2 713(6)   | 1 754(25)  | 3 137(9)   | C(715) | 2 011(7)  | 3 835(28)  | 5 148(12) |
| C(321) | 2 335(6)   | 269(19)    | 2 914(7)   | C(716) | 1 772(10) | 3 365(18)  | 5 098(12) |
| C(322) | 2 083(6)   | 504(16)    | 2 681(10)  | C(721) | 1 168(8)  | 2 750(25)  | 5 408(12) |
| C(323) | 2 025(5)   | 261(19)    | 2 261(9)   | C(722) | 995(7)    | 2 098(23)  | 5 447(12) |
| C(324) | 2 217(7)   | -216(20)   | 2 075(7)   | C(723) | 930(8)    | 1 863(22)  | 5 840(16) |
| C(325) | 2 468(6)   | -451(18)   | 2 309(11)  | C(724) | 1 039(11) | 2 281(33)  | 6 194(11) |
| C(326) | 2 527(5)   | -208(20)   | 2 729(10)  | C(725) | 1 212(10) | 2 934(31)  | 6 156(13) |
| C(331) | 2 600(8)   | -158(21)   | 3 682(11)  | C(726) | 1 277(8)  | 3 169(22)  | 5 763(17) |
| C(332) | 2 890(8)   | -125(21)   | 3 707(12)  | C(731) | 932(5)    | 3 664(16)  | 4 728(10) |
| C(333) | 3 051(6)   | -752(29)   | 3 890(13)  | C(732) | 758(7)    | 3 992(19)  | 5 002(7)  |
| C(334) | 2 921(10)  | -1 410(24) | 4 047(13)  | C(733) | 531(6)    | 4 461(19)  | 4 847(10) |
| C(335) | 2 631(11)  | -1 443(21) | 4 021(13)  | C(734) | 478(5)    | 4 602(18)  | 4 418(11) |
| C(336) | 2 470(6)   | -816(26)   | 3 838(13)  | C(735) | 651(7)    | 4 275(20)  | 4 144(8)  |
| C(411) | 1 197(5)   | -2 496(18) | 4 683(10)  | C(736) | 878(6)    | 3 805(18)  | 4 299(9)  |
| C(412) | 939(7)     | -2 158(14) | 4 728(10)  | C(811) | 590(6)    | 612(17)    | 2 853(11) |
| C(413) | 700(5)     | -2 624(20) | 4 679(10)  | C(812) | 642(6)    | -95(23)    | 3 072(8)  |
| C(414) | 718(6)     | -3 428(19) | 4 585(11)  | C(813) | 543(8)    | -811(16)   | 2 896(12) |

Table 2 (continued)

| Atom   | X/a    | Y/b       | Z/c       | Atom   | X/a      | Y/b       | Z/c       |
|--------|--------|-----------|-----------|--------|----------|-----------|-----------|
| C(814) | 393(7) | -820(19)  | 2 500(13) | C(826) | 397(6)   | 2 751(19) | 3 367(11) |
| C(815) | 342(7) | -113(27)  | 2 280(9)  | C(831) | 815(7)   | 2 116(19) | 2 670(9)  |
| C(816) | 440(7) | 603(19)   | 2 457(11) | C(832) | 636(5)   | 2 651(19) | 2 445(10) |
| C(821) | 399(6) | 1 950(20) | 3 256(10) | C(833) | 726(6)   | 3 070(17) | 2 113(9)  |
| C(822) | 166(7) | 1 471(15) | 3 308(10) | C(834) | 995(7)   | 2 954(20) | 2 004(9)  |
| C(823) | -69(6) | 1 793(21) | 3 471(11) | C(835) | 1 174(5) | 2 419(21) | 2 229(11) |
| C(824) | -71(6) | 2 595(22) | 3 581(11) | C(836) | 1 084(6) | 2 000(18) | 2 561(11) |
| C(825) | 162(8) | 3 074(15) | 3 530(12) |        |          |           |           |

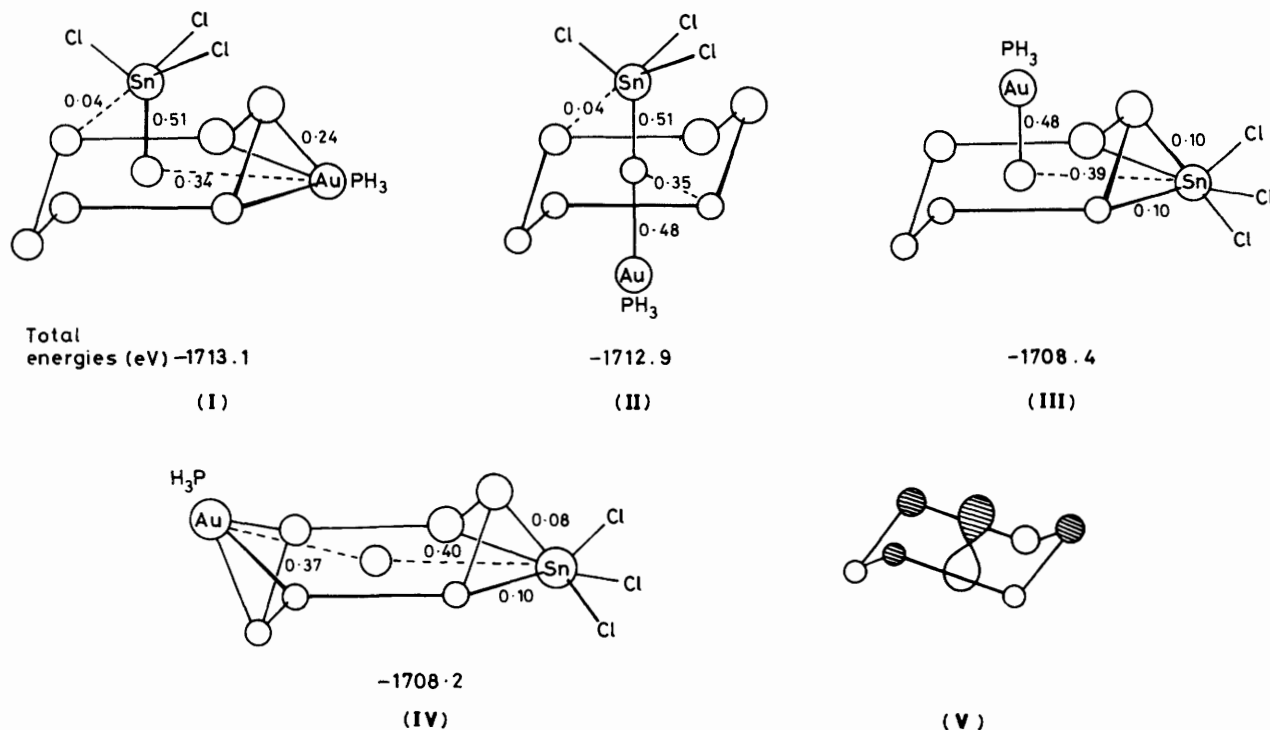
Table 3. Bond lengths (Å) and angles (°) for  $[\text{Au}_8(\text{PPh}_3)_7(\text{SnCl}_3)]_2[\text{SnCl}_6]$ 

| Central gold atom |           |                   |           | Peripheral gold atoms               |           |                     |           |
|-------------------|-----------|-------------------|-----------|-------------------------------------|-----------|---------------------|-----------|
| Au(1)-Au(2)       | 2.648(2)  | Au(1)-Au(3)       | 2.640(2)  | Au(2)-Au(3)                         | 2.872(2)  | Au(2)-Au(4)         | 2.904(2)  |
| Au(1)-Au(4)       | 2.664(2)  | Au(1)-Au(5)       | 2.672(2)  | Au(3)-Au(5)                         | 2.912(2)  | Au(4)-Au(6)         | 2.847(2)  |
| Au(1)-Au(6)       | 2.640(2)  | Au(1)-Au(7)       | 2.679(2)  | Au(5)-Au(7)                         | 2.945(2)  | Au(5)-Au(8)         | 2.900(2)  |
| Au(1)-Au(8)       | 2.633(2)  | Au(1)-Sn(1)       | 2.625(3)  | Au(6)-Au(7)                         | 2.940(2)  | Au(6)-Au(8)         | 2.881(3)  |
|                   |           |                   |           | Au(7)-Au(8)                         | 2.965(3)  |                     |           |
| Metal-ligand      |           |                   |           | Disordered hexachlorostannate anion |           |                     |           |
| Au(2)-P(2)        | 2.29(1)   | Au(3)-P(3)        | 2.29(1)   | Sn(2)-Cl(21)                        | 2.37(3)   | Sn(2)-Cl(22)        | 2.42(4)   |
| Au(4)-P(4)        | 2.31(1)   | Au(5)-P(5)        | 2.29(1)   | Sn(2)-Cl(23)                        | 2.53(3)   | Sn(2)-Cl(24)        | 2.52(3)   |
| Au(6)-P(6)        | 2.28(1)   | Au(7)-P(7)        | 2.28(1)   | Sn(3)-Cl(31)                        | 2.41(4)   | Sn(3)-Cl(32)        | 2.44(4)   |
| Au(8)-P(8)        | 2.27(1)   |                   |           | Sn(3)-Cl(33)                        | 2.43(5)   | Sn(3)-Cl(34)        | 2.46(5)   |
| Sn(1)-Cl(11)      | 2.42(1)   | Sn(1)-Cl(12)      | 2.40(1)   | Sn(3)-Cl(35)                        | 2.45(4)   | Sn(3)-Cl(36)        | 2.35(5)   |
| Sn(1)-Cl(13)      | 2.46(1)   |                   |           |                                     |           |                     |           |
| Au(3)-Au(1)-Au(2) | 65.79(6)  | Au(4)-Au(1)-Au(2) | 66.30(6)  | P(6)-Au(6)-Au(1)                    | 178.5(3)  | P(6)-Au(6)-Au(4)    | 123.2(3)  |
| Au(4)-Au(1)-Au(3) | 105.90(7) | Au(5)-Au(1)-Au(2) | 110.07(8) | P(6)-Au(6)-Au(7)                    | 121.4(3)  | P(6)-Au(6)-Au(8)    | 122.9(3)  |
| Au(5)-Au(1)-Au(3) | 66.49(6)  | Au(5)-Au(1)-Au(4) | 172.28(8) | Au(5)-Au(7)-Au(1)                   | 56.51(6)  | Au(6)-Au(7)-Au(1)   | 55.82(6)  |
| Au(6)-Au(1)-Au(2) | 100.18(7) | Au(6)-Au(1)-Au(3) | 165.88(9) | Au(6)-Au(7)-Au(5)                   | 104.85(7) | Au(8)-Au(7)-Au(1)   | 55.34(6)  |
| Au(6)-Au(1)-Au(4) | 64.93(6)  | Au(6)-Au(1)-Au(5) | 122.79(8) | Au(8)-Au(7)-Au(5)                   | 58.78(6)  | Au(8)-Au(7)-Au(6)   | 58.41(6)  |
| Au(7)-Au(1)-Au(2) | 157.57(9) | Au(7)-Au(1)-Au(2) | 126.57(8) | P(7)-Au(7)-Au(1)                    | 163.3(3)  | P(7)-Au(7)-Au(5)    | 124.3(3)  |
| Au(7)-Au(1)-Au(4) | 119.33(8) | Au(7)-Au(1)-Au(5) | 66.77(6)  | P(7)-Au(7)-Au(6)                    | 130.1(3)  | P(7)-Au(7)-Au(8)    | 141.1(3)  |
| Au(7)-Au(1)-Au(6) | 67.11(6)  | Au(8)-Au(1)-Au(2) | 90.30(8)  | Au(5)-Au(8)-Au(1)                   | 57.52(6)  | Au(6)-Au(8)-Au(1)   | 56.99(6)  |
| Au(8)-Au(1)-Au(3) | 113.43(8) | Au(8)-Au(1)-Au(4) | 119.69(8) | Au(6)-Au(8)-Au(5)                   | 107.55(7) | Au(7)-Au(8)-Au(1)   | 56.80(6)  |
| Au(8)-Au(1)-Au(5) | 66.27(7)  | Au(8)-Au(1)-Au(6) | 66.24(7)  | Au(7)-Au(8)-Au(5)                   | 60.26(6)  | Au(7)-Au(8)-Au(6)   | 60.36(6)  |
| Au(8)-Au(1)-Au(7) | 67.86(7)  | Sn(1)-Au(1)-Au(2) | 119.56(9) | P(8)-Au(8)-Au(1)                    | 161.2(3)  | P(8)-Au(8)-Au(5)    | 129.1(3)  |
| Sn(1)-Au(1)-Au(3) | 80.36(9)  | Sn(1)-Au(1)-Au(4) | 78.11(9)  | P(8)-Au(8)-Au(6)                    | 123.0(3)  | P(8)-Au(8)-Au(7)    | 141.6(3)  |
| Sn(1)-Au(1)-Au(5) | 98.75(9)  | Sn(1)-Au(1)-Au(6) | 106.90(9) |                                     |           |                     |           |
| Sn(1)-Au(1)-Au(7) | 82.53(9)  | Sn(1)-Au(1)-Au(8) | 150.1(1)  | Cl(11)-Sn(1)-Au(1)                  | 117.8(3)  | Cl(12)-Sn(1)-Au(1)  | 121.4(3)  |
| Au(3)-Au(2)-Au(1) | 56.97(6)  | Au(4)-Au(2)-Au(1) | 57.11(6)  | Cl(12)-Sn(1)-Cl(11)                 | 95.7(4)   | Cl(13)-Sn(1)-Au(1)  | 123.0(3)  |
| Au(4)-Au(2)-Au(3) | 94.24(7)  | P(2)-Au(2)-Au(1)  | 169.9(3)  | Cl(13)-Sn(1)-Cl(11)                 | 97.1(4)   | Cl(13)-Sn(1)-Cl(12) | 95.7(4)   |
| P(2)-Au(2)-Au(3)  | 128.3(3)  | P(2)-Au(2)-Au(4)  | 126.4(3)  |                                     |           |                     |           |
| Au(2)-Au(3)-Au(1) | 57.24(6)  | Au(5)-Au(3)-Au(1) | 57.29(6)  | Cl(22)-Sn(2)-Cl(21)                 | 180.00    | Cl(23)-Sn(2)-Cl(21) | 88.0(6)   |
| Au(5)-Au(3)-Au(2) | 97.84(7)  | P(3)-Au(3)-Au(1)  | 172.3(3)  | Cl(23)-Sn(2)-Cl(22)                 | 92.0(6)   | Cl(23)-Sn(2)-Cl(23) | 175.9(13) |
| P(3)-Au(3)-Au(2)  | 122.3(3)  | P(3)-Au(3)-Au(5)  | 128.8(3)  | Cl(24)-Sn(2)-Cl(21)                 | 88.4(7)   | Cl(24)-Sn(2)-Cl(22) | 91.6(7)   |
| Au(2)-Au(4)-Au(1) | 56.59(6)  | Au(6)-Au(4)-Au(1) | 57.13(6)  | Cl(24)-Sn(2)-Cl(23)                 | 85.6(11)  | Cl(24)-Sn(2)-Cl(23) | 94.2(11)  |
| Au(6)-Au(4)-Au(2) | 89.69(7)  | P(4)-Au(4)-Au(1)  | 168.1(3)  |                                     |           |                     |           |
| P(4)-Au(4)-Au(2)  | 126.9(3)  | P(4)-Au(4)-Au(6)  | 130.7(3)  | Cl(32)-Sn(3)-Cl(31)                 | 177.9(15) | Cl(33)-Sn(3)-Cl(32) | 89.1(16)  |
| Au(3)-Au(5)-Au(1) | 56.22(6)  | Au(7)-Au(5)-Au(1) | 56.71(6)  | Cl(33)-Sn(3)-Cl(32)                 | 90.2(17)  | Cl(34)-Sn(3)-Cl(31) | 89.1(18)  |
| Au(7)-Au(5)-Au(3) | 108.41(7) | Au(8)-Au(5)-Au(1) | 56.22(6)  | Cl(34)-Sn(3)-Cl(32)                 | 88.9(18)  | Cl(34)-Sn(3)-Cl(33) | 87.8(18)  |
| Au(8)-Au(5)-Au(3) | 98.64(7)  | Au(8)-Au(5)-Au(7) | 60.96(6)  | Cl(35)-Sn(3)-Cl(31)                 | 90.3(14)  | Cl(35)-Sn(3)-Cl(32) | 91.7(15)  |
| P(5)-Au(5)-Au(1)  | 177.3(3)  | P(5)-Au(5)-Au(3)  | 124.5(3)  | Cl(35)-Sn(3)-Cl(33)                 | 91.0(16)  | Cl(35)-Sn(3)-Cl(34) | 178.6(16) |
| P(5)-Au(5)-Au(7)  | 121.4(3)  | P(5)-Au(5)-Au(8)  | 125.2(3)  | Cl(36)-Sn(3)-Cl(31)                 | 91.4(17)  | Cl(36)-Sn(3)-Cl(32) | 89.3(17)  |
| Au(4)-Au(6)-Au(1) | 57.94(6)  | Au(7)-Au(6)-Au(1) | 57.08(6)  | Cl(36)-Sn(3)-Cl(33)                 | 179.5(18) | Cl(36)-Sn(3)-Cl(34) | 92.2(18)  |
| Au(7)-Au(6)-Au(4) | 105.64(7) | Au(8)-Au(6)-Au(1) | 56.77(6)  | Cl(36)-Sn(3)-Cl(35)                 | 89.0(16)  |                     |           |
| Au(8)-Au(6)-Au(4) | 106.18(7) | Au(8)-Au(6)-Au(7) | 61.24(6)  |                                     |           |                     |           |

*Theoretical Analysis.*—Molecular-orbital calculations on high-nuclearity gold cluster compounds of the general type  $[\text{Au}(\text{AuPH}_3)_n]^{2+}$  have demonstrated that they can be classified into two broad topological classes according to the three-dimensional disposition of the peripheral gold atoms. If they lie on a spherical surface they are characterised by a total of  $12n + 18$  valence electrons, but if they adopt a toroidal or elliptical arrangement the total number of valence electrons is  $12n + 16$ .<sup>20-22</sup> All the spherical clusters are derived from a

centred chair,  $[\text{Au}_7(\text{PR}_3)_6]^+$ , and have either  $\text{AuPR}_3$  or triangular  $\text{Au}_3(\text{PR}_3)_3$  fragments co-ordinated to it along the three-fold symmetry axis. In contrast those toroidal clusters derived from the centred chair have the  $\text{AuPR}_3$  fragments bridging edge Au-Au bonds. Since the removal of two opposite triangular faces from an icosahedron also leads to a hexagonal chair the majority of gold cluster compounds can also be described in terms of fragments of icosahedra.

The  $[\text{Au}_8(\text{PPh}_3)_7]^{2+}$  cluster has a total of  $12n + 16$ , i.e. 112,



Scheme 2. The overlap populations are shown adjacent to the bonds to which they refer

valence electrons and a typical toroidal geometry based on an edge-bridged hexagonal  $[\text{Au}_7(\text{PPh}_3)_6]^+$  structure [see (IIb) in Scheme 1]. Addition of  $\text{PPh}_3$  to (IIb) results in the formation of  $[\text{Au}_8(\text{PPh}_3)_7]^{2+}$  [(II) in Scheme 1], which has a total of  $12n + 18$ , i.e. 114, valence electrons. The movement of an  $\text{AuPPh}_3$  fragment to an axial position and the co-ordination of  $\text{PPh}_3$  to the central gold atom and *trans* to this  $\text{AuPPh}_3$  fragment leads to a cluster with a pseudo-spherical topology if  $\text{AuPPh}_3$  and  $\text{PPh}_3$  are considered as constituents of the polyhedron and pseudo-hemispherical if only the gold atoms are considered.

The addition of  $\text{SnCl}_3^-$  to  $[\text{Au}_8(\text{PPh}_3)_7]^{2+}$  to give  $[\text{Au}_8(\text{PPh}_3)_7(\text{SnCl}_3)]^+$  (I) also leads to an increase in the valence electron count from 112 to 114. The structure of (I) as determined by the single-crystal study is represented in Scheme 2 as (I). Some alternative structures, (II)–(IV), for the gold-tin cluster are also shown in Scheme 2. Extended-Hückel molecular-orbital calculations (see refs. 20–22 for details of the type of calculation used and the relevant parameters) have been completed on (I)–(IV) in order to account for the observed preference for (I). The calculated total energies for (III) and (IV) shown in the Scheme are clearly much higher ( $\approx 5$  eV) than those for the other structures shown and it is clearly unfavourable for the  $\text{SnCl}_3$  group to bond to the  $[\text{Au}_7(\text{PH}_3)_6]^+$  in an edge-bridging fashion. The overlap between the out-pointing  $\text{SnCl}_3$  hybrid orbital and a sequence of three gold atoms which it is edge bridging is very unfavourable and is a major contributor to the large energy difference between (III) and (IV) and (I) and (II). The  $[\text{Au}_7(\text{PH}_3)_6]^+$  moiety has as its lowest unoccupied molecular orbital (l.u.m.o.) an orbital of  $a_{2u}$  symmetry which is illustrated in (V) of Scheme 2.<sup>20</sup> This orbital has a substantial contribution from the  $6p_z$  orbital of the central gold atom and is exceptionally well set-up to interact strongly with the donor orbital of the in-coming  $\text{SnCl}_3$  ligand. The large Au–Sn overlap population computed for (I) and (II) and shown in the Scheme confirms the strength of this interaction.

The overlap between the out-pointing hybrid orbital of  $\text{AuPH}_3$  and the gold atoms of the  $[\text{Au}_7(\text{PH}_3)_6]^+$  moiety is less

sensitive to its precise location. For example, (I) and (II) which have  $\text{AuPH}_3$  located either axially, (II), or edge bridging, (I), have very similar energies. Interestingly the calculations confirm that the observed structure for  $[\text{Au}_8(\text{PPh}_3)_7(\text{SnCl}_3)]^+$  (I) is the most stable, but only by *ca.* 0.2 eV. Therefore, the apparent stereochemical non-rigidity of (I) indicated by the variable-temperature  $^{31}\text{P}$  n.m.r. studies is consistent with the occurrence of a second symmetrical structure such as (II) with a similar total energy.

In summary the adoption of a hemi-spherical topology by  $[\text{Au}_8(\text{PPh}_3)_7(\text{SnCl}_3)]^+$  (I) arises because this geometry permits a strong interaction between the  $\text{SnCl}_3$  'lone pair' orbital and the  $a_{2u}$  molecular orbital of the hexagonal  $[\text{Au}_7(\text{PPh}_3)_6]^+$  moiety. The additional  $\text{AuPPh}_3^+$  fragment can either edge bridge this structure to give (I) or at slightly higher energy cap the structure to give a spherical topology. The small energy difference between these alternative structures provides an explanation for the stereochemical non-rigidity of the compound.

### Experimental

Reactions involving  $\text{NET}_4\text{SnCl}_3$  were carried out using standard Schlenk-line procedures under an atmosphere of pure, dry  $\text{N}_2$  and using dry  $\text{O}_2$ -free solvents. Otherwise no special precautions were taken to exclude air or moisture from the synthetic procedures. Microanalyses were carried out by Mr. M. Gascoyne and his staff at this laboratory.

Proton-decoupled  $^{31}\text{P}\{-^1\text{H}\}$  n.m.r. spectra were recorded on a Bruker AM-250 spectrometer and the samples were referenced to  $\text{PO}(\text{OCH}_3)_3$  in  $\text{D}_2\text{O}$ . The machine operating frequency was 101.26 MHz.

The compounds  $[\text{Au}_9(\text{PPh}_3)_8][\text{NO}_3]_3$ ,  $[\text{Au}_8(\text{PPh}_3)_8][\text{NO}_3]_2$ , and  $[\text{Au}_8(\text{PPh}_3)_7][\text{NO}_3]_2$  were synthesised by literature methods.<sup>10,11,17,18</sup>

The  $^{119}\text{Sn}$  Mössbauer spectra were kindly recorded for us by Dr. Peter Smith of the International Tin Research Institute, Uxbridge. The spectra were measured at 80 K using a constant-

acceleration microprocessor Mössbauer spectrometer. The experimental errors in the isomer shifts and quadrupole splittings are  $\pm 0.05 \text{ mm s}^{-1}$ .

*Syntheses of  $[\text{Au}_8(\text{PPh}_3)_7(\text{SnCl}_3)_2][\text{SnCl}_6]$ .*—(a) From  $[\text{Au}_9(\text{PPh}_3)_8][\text{NO}_3]_3$ . The compound  $[\text{Au}_9(\text{PPh}_3)_8][\text{NO}_3]_3$  (0.2 g) was suspended in acetone ( $10 \text{ cm}^3$ ) and  $\text{SnCl}_2 \cdot 2\text{H}_2\text{O}$  (0.1 g) was added with stirring. The green suspension turned red and a red precipitate began to separate after 3 min. After 2.5 h the red precipitate was filtered off, washed well with acetone, and dried under vacuum (ca. 80% yield based on gold). Red crystals of  $[\text{Au}_8(\text{PPh}_3)_7(\text{SnCl}_3)_2][\text{SnCl}_6]$  (1) were obtained on layering a solution of  $\text{CH}_2\text{Cl}_2$  with benzene.

(b) From  $[\text{Au}_8(\text{PPh}_3)_7][\text{NO}_3]_2$ . The compound  $[\text{Au}_8(\text{PPh}_3)_7][\text{NO}_3]_2$  (0.2 g) was dissolved in acetone ( $25 \text{ cm}^3$ ) and  $\text{SnCl}_2 \cdot 2\text{H}_2\text{O}$  (0.1 g) was added with stirring. The solution became orange-red immediately and an orange precipitate separated out. After 0.5 h the precipitate was filtered off and washed well with acetone (ca. 90% yield based on gold). Red crystals of  $[\text{Au}_8(\text{PPh}_3)_7(\text{SnCl}_3)_2][\text{SnCl}_6]$  suitable for X-ray diffraction studies were obtained from  $\text{CH}_2\text{Cl}_2$ -hexane.

(c) From  $[\text{Au}_8(\text{PPh}_3)_8][\text{NO}_3]_2$  and  $\text{NEt}_4\text{SnCl}_3$ . The compound  $[\text{Au}_8(\text{PPh}_3)_8][\text{NO}_3]_2$  (0.18 g) was dissolved in acetone ( $20 \text{ cm}^3$ ) and  $\text{NEt}_4\text{SnCl}_3$  (0.072 g, 4 mol equivalents) was added and the solution stirred for 0.5 h. The solution lightened in colour and an orange-red precipitate separated out. After filtration and washing with acetone, red crystals of  $[\text{Au}_8(\text{PPh}_3)_7(\text{SnCl}_3)_2][\text{SnCl}_6]$  were obtained from  $\text{CH}_2\text{Cl}_2$ -hexane.

The samples obtained from the alternative synthetic routes (a)–(c) were shown to be identical by single-crystal X-ray studies which established that the crystalline samples were isomorphous. Satisfactory analytical data were obtained for the samples. A representative analysis: C, 38.7; H, 2.8; Cl, 5.6.  $\text{C}_{252}\text{H}_{210}\text{Au}_{16}\text{Cl}_{12}\text{P}_{14}\text{Sn}_3$  requires C, 39.8; H, 2.8; Cl, 5.6%.

*Crystal Structure Determination.*—Crystals of  $[\text{Au}_8(\text{PPh}_3)_7(\text{SnCl}_3)_2][\text{SnCl}_6]$  (1) were grown from  $\text{CH}_2\text{Cl}_2$ -hexane and a plate-like crystal of dimensions  $0.4 \times 0.35 \times 0.1 \text{ mm}$  was mounted in a 0.5-mm capillary tube. Details of the X-ray crystallographic analysis are summarised in Table 1. The intensity data were collected on an Enraf-Nonius CAD4-F diffractometer using graphite-monochromated Mo- $K_\alpha$  radiation. Corrections were made to the intensity data for crystal decomposition (to 60% of the original intensities) and an empirical absorption correction based on an azimuthal scan was applied (maximum and minimum corrections 1.8–1.0).

Those reflections which overlapped were omitted from the refinement. 11 747 Unique reflections were measured in the  $2\theta$  range 3–45°.

The structure was solved using the MITHRIL<sup>23,24</sup> direct-methods program, which gave the positions of the eight gold atoms. All remaining non-hydrogen atoms were obtained from successive Fourier difference syntheses and least-squares refinements. These calculations were completed using the CRYSTALS suite of programs.<sup>24</sup> The phenyl rings were refined as restrained groups with C–C 1.395 Å. The metal atoms in the cations were refined with anisotropic thermal parameters; the remaining atoms were refined isotropically and the hydrogen atoms were included by locating them at their calculated positions. In the final cycles of the least-squares refinement the  $\text{SnCl}_6^{2-}$  anion which had initially been located on the two-fold axis was found to have unreasonably high thermal parameters and inspection of a Fourier difference map showed the presence of a peak of intensity  $6.0 \text{ e} \text{ \AA}^{-3}$  at  $3.0 \text{ \AA}$  from the tin position. It proved necessary to refine the  $\text{SnCl}_6^{2-}$  anion as a disordered group in three orientations with components on and off the two-fold axis. Alternative refinements based for example on

$\text{Sn}_2\text{Cl}_{10}^{2-}$  proved to be less satisfactory and led to unreasonable Sn–Sn distances. It has been noted<sup>25</sup> that the addition of  $\text{SnCl}_2$  to  $[\text{AgCl}(\text{PPh}_3)_3]$  results in the formation of  $[\text{Ag}(\text{PPh}_3)_4]^+ \text{OH}^- [\text{SnCl}_3(\text{OH})(\text{H}_2\text{O})]_2$ . The presence of the neutral dimeric tin product was suggested by the Mössbauer data, and it has been formulated as a dimeric species based on octahedral tin atoms and which are linked by the hydroxo-bridges. The presence of this dimer was attributed to an ageing process in  $\text{SnCl}_2$  solutions. Since the Mössbauer isomer shift for this dimer is very similar to that observed in (1) the peaks attributed to the disordered  $\text{SnCl}_6^{2-}$  anion were re-examined in order to establish whether they were consistent with the presence of such a dimer. However, a satisfactory model could not be established. Therefore, the  $\text{SnCl}_6^{2-}$  anion was found to be most consistent with the observed electron density.

Additional material available from the Cambridge Crystallographic Data Centre comprises thermal parameters and remaining bond lengths and angles.

### Acknowledgements

The S.E.R.C. is thanked for financial support and Johnson Matthey Ltd. for a generous loan of gold metal.

### References

- 1 K. P. Hall and D. M. P. Mingos, *Prog. Inorg. Chem.*, 1984, **32**, 238.
- 2 D. M. P. Mingos, *Gold Bull.*, 1984, **17**, 5.
- 3 J. J. Steggerda, *Recl. Trav. Chim. Pays-Bas*, 1982, **101**, 164.
- 4 W. Bos, J. J. Bour, J. W. A. van der Velden, J. J. Steggerda, A. L. Cassalnuovo, and L. H. Pignolet, *J. Organomet. Chem.*, 1983, **253**, C64.
- 5 J. W. A. van der Velden, J. J. Bour, J. J. Steggerda, P. T. Beurskens, M. Roseboom, and J. H. Noordik, *Inorg. Chem.*, 1982, **21**, 4321.
- 6 C. E. Briant, B. R. C. Theobald, J. W. White, L. K. Bell, and D. M. P. Mingos, *J. Chem. Soc., Chem. Commun.*, 1981, 201.
- 7 F. Demartin, M. Manassero, L. Naldini, R. Ruggeri, and M. Sansoni, *J. Chem. Soc., Chem. Commun.*, 1981, 222.
- 8 J. W. A. van der Velden, J. J. Bour, B. F. Otterloo, W. P. Bosman, and J. H. Noordik, *J. Chem. Soc., Chem. Commun.*, 1981, 583.
- 9 L. Malatesta, L. Naldini, G. Simonetta, and F. Cariati, 'Proceedings Bressanone Conference, 1965,' Elsevier, New York, 1966.
- 10 F. Cariati and L. Naldini, *J. Chem. Soc., Dalton Trans.*, 1972, 2286.
- 11 J. W. A. van der Velden, J. J. Bour, W. P. Bosman, and J. H. Noordik, *J. Chem. Soc., Chem. Commun.*, 1981, 1218.
- 12 N. J. Clayden, C. M. Dobson, K. P. Hall, D. M. P. Mingos, and D. J. Smith, *J. Chem. Soc., Dalton Trans.*, 1985, 1811.
- 13 N. N. Greenwood and T. C. Gibb, 'Mössbauer Spectroscopy,' Chapman and Hall, London, 1977.
- 14 M. J. Mays and P. L. Sears, *J. Chem. Soc., Dalton Trans.*, 1974, 2254.
- 15 J. W. A. van der Velden, J. J. Bour, W. P. Bosman, and J. H. Noordik, *J. Chem. Soc., Chem. Commun.*, 1981, 1218.
- 16 W. Clegg, *Acta Crystallogr., Sect. B*, 1978, **34**, 278.
- 17 M. Manassero, L. Naldini, and M. Sansoni, *J. Chem. Soc., Chem. Commun.*, 1979, 385.
- 18 F. A. Vollenbroek, J. J. Bour, W. P. Bosman, J. H. Noordik, and P. T. Beurskens, *J. Chem. Soc., Chem. Commun.*, 1979, 387.
- 19 M. R. Churchill and K. K. G. Lin, *J. Am. Chem. Soc.*, 1974, **96**, 76.
- 20 K. P. Hall, D. I. Gilmour, and D. M. P. Mingos, *J. Organomet. Chem.*, 1984, **268**, 275.
- 21 D. M. P. Mingos, *J. Chem. Soc., Dalton Trans.*, 1976, 1163.
- 22 D. M. P. Mingos, *Proc. R. Soc. London, Ser. A*, 1982, **308**, 75.
- 23 C. J. Gilmore, MITHRIL, University of Glasgow, 1984.
- 24 D. J. Watkin, J. R. Caruthers, and B. W. Betteridge, CRYSTALS User Guide, Chemical Crystallography Laboratory, University of Oxford, 1985.
- 25 D. V. Sanghani, P. J. Smith, D. W. Allen, and B. F. Taylor, *Inorg. Chim. Acta*, 1982, **59**, 203.